Combination of Fractal Geometry and Hydrodynamics: A Novel Approach to the Study of a Multicapillary Electrophoresis System

Yves Claude Guillaume,* Eric Peyrin, and Christiane Guinchard

Laboratoire de Chimie Analytique, Faculté de Médecine et Pharmacie, Place St. Jacques, 25030 Besançon, Cedex, France

Received: November 18, 1998; In Final Form: April 22, 1999

In this paper, the effect of the capillary structure and its organization in a multicapillary electrophoresis system (MES) were studied. The model was based on a combination of the dynamics of energy transport and the mathematics of fractal geometry. It demonstrated that in order to minimize the energy transport the geometric system structure must obey certain power laws. The results obtained showed that these power laws depend on the hydrodynamic regime and the capillary material. For polymeric capillaries in a pulsed flow, the viscous resistance in the fractal multicapillary system (FMS) varied with $1/r^2$ for the smallest capillaries (r was the dimension of the capillary cross-section) and with $1/r^4$ (Poiseuille flow regime) for the largest capillaries. For a constant flow, the Poiseuille regime was always respected. The FMS can use high field strengths without too much energy dissipation to perform rapid and efficient separation.

Introduction

In recent years, studies on tapered capillaries with a non uniform cross-section[1] and capillaries with a rectangular cross-section[2,3] have been carried out. Relationships governing hydrodynamic flow, plate height, thermal dissipation, analysis speed, and sample capacity have been detailed by Cifuentes and Poppe[3], and the advantages and drawbacks for the routine use of rectangular cross-section capillaries discussed. Other studies have been conducted to investigate the effect of geometry and capillary organization. Fused-silica capillaries with microconcentric[4] and tapered shapes[5] have been used. The construction of the microconcentric columns by Fujimoto and co-workers[4] involved helically winding a plastic line around a small-diameter fused-silica capillary and then inserting this unit into a larger diameter capillary. It was reported that this configuration afforded higher sample loading than had been possible with conventional CE, and its utility in a micropreparative application was explored. Burggraf and co-workers[6−8] developed a novel CE-based column swatching system on a planar glass structure that they referred to as synchronized cyclic capillary electrophoresis (SCCE). This structure was composed of four 20-mm long capillaries arranged in a square. The authors reported moving one component around the system (one cycle) in 1 min with 2.5 kV and evaluated peak dispersion during this process.[8] The nature of the capillary material was also discussed. Fused silica has long been the standard material for capillary separations. Recently, several studies have focused on the use of polypropylene capillaries as analytical separation tubes for CE.[9−12] Hollow polypropylene fibers wall-modified with dextran,[9] cellulose,[11] and ionic functional groups (sulfonic acid, quaternary amine, substituted polyphosphazene)[10] have been investigated to ascertain their utility for protein, peptide, and nucleic acid separations. Fridstroem and co-workers[12] have also demonstrated bare and surface-modified polypropylene for MEKC. Other materials that have recently been investigated include hollow polymethacrylate fibers[13] and capillaries formed from poly(butylene, terephthalate), ethylene/vinyl acetate, and nylon[14] as well as fluorinated ethylene−propylene copolymers.[15] The modulation response of the physical parameters has also been examined for CE separations. To extend the range of resolution pulsed-field techniques (with and without field inversion) which allow the DNA strands to revert back, momentarily, to the coiled structure in which mobility is more precisely related to molecular weight,[16−20] Kim and Morris[18] demonstrated the resolution of DNA by applying rapid pulse electric fields. Sudor and Novotny[20] evaluated the relationship between the mobility of duplex DNA (5−100 kb) in neutral polymer networks and the frequency and pulse shape of the applied voltage. The aim of this paper was to make a theoretical analysis of a multicapillary electrophoresis system (MES) in terms of its geometry and hydrodynamics. Fractal geometry pioneered by the physicist Benoit Mandelbrot was used. The effect of the elastic and pulsatile nature of the polymeric capillaries on the hydrodynamic regime of the system was also assessed.

Geometrical Characteristics of the Fractal Multicapillary System

To define the fractal multicapillary system (FMS), one major assumption is that a minimum amount of energy is required to transport the background electrolyte (BGE) in the FMS. Fractal geometry (FG) which has been used to model many seemingly natural structures was used to investigate energy transfer. The FMS is composed of branching from the capillary with the highest cross-section (level 0) to the lowest (level s) (Figure 1). Each capillary ramifies into n_l smaller ones. At level l the capillary has a square cross-section on one side r_l or a circular cross-section of a radius r_l. The capillary length is L_l.

The parameters

$$a_l = r_{l+1}/r_l \tag{1}$$

and

$$b_l = L_{l+1}/L_l \tag{2}$$

10.1021/jp984475c CCC: $18.00
Published on Web 06/11/1999

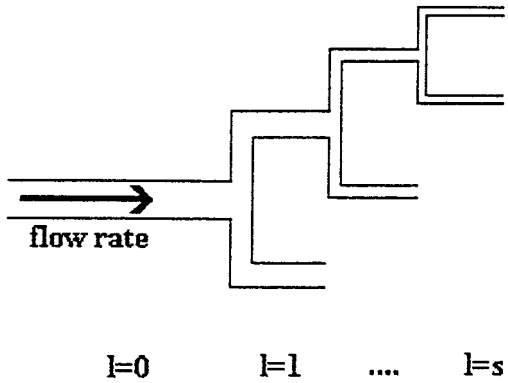

Figure 1. Representation of the fractal multicapillary system (FMS). Here, l is the order of the level, beginning with the capillaries with the largest cross-section ($l = 0$) and ending with those with the smallest cross-section ($l = s$).

were introduced to characterize the ramifications of the FMS. As the FMS has a self-similar fractal nature, this implies that a_l, b_l, and n_l must be independent of l: $a_l = a$ = constant; $b_l = b$ = constant; $n_l = n$ = constant. So at level l, the total number of capillaries can be expressed as

$$N_l = n^l \tag{3}$$

At level l, the volume of the background electrolyte (BGE) in one capillary was

$$V_l = \lambda r_l^2 L_l \tag{4}$$

$\lambda = 1$ for capillaries with a rectangular cross-section and $\lambda = \pi$ for a circular section.

Thus, the total volume V_t of BGE in the FMS system was

$$V_t = \sum_{l=o}^{s} V_l N_l \tag{5}$$

Combining eqs 3, 4, and 5 gives

$$V_t = \sum_{l=o}^{s} \lambda {r_1}^2 L_l n^l \tag{6}$$

which yields

$$V_t = \frac{(na^2b)^{-(s+1)} - 1}{(na^2b)^{-1} - 1} \times n^s V_s \tag{7}$$

where V_s denoted the BGE volume in the smallest capillaries (level s). This latter equation reflects the fractal nature of the system.

Hydrodynamic Study

If U is the voltage across the FMS, then the electric field strength is given by

$$E = U/\sum_{l=o}^{s} L_l \tag{8}$$

Combining eqs 2 and 8 gives

$$E = U/\left(\frac{b^{-(s+1)} - 1}{b^{-1} - 1} L_s\right) \tag{9}$$

where L_s denotes the length of the smallest capillary.

At level l, the electroosmotic flow velocity is

$$v_{\mathrm{eos},l} = u_{\mathrm{eos},l} E \tag{10}$$

where $u_{\mathrm{eos},l}$ is the electroosmotic flow mobility at level l, and the corresponding flow rate was

$$F_{\mathrm{eos},l} = u_{\mathrm{eos},l}\, E\, \lambda {r_1}^2 \tag{11}$$

As BGE is maintained as it flows through the FMS,

$$F_{\mathrm{eos},o} = N_l F_{\mathrm{eos},l} = N_s F_{\mathrm{eos},s} \tag{12}$$

Flow kinetics for capillaries have been described in detail by several authors.[21,23] Lucas[21] and Washburn[22] used a theoretical approach that was based on a fully developed laminar flow of a Newtonian liquid with negligible inertia effects. For a steady laminar flow, the viscous resistance R_l of the capillary at level l can be given by the well-known Poiseuille relation[24]

$$R_l = 8\eta L_l/\pi {r_1}^4 \tag{13}$$

where η is the viscosity of the BGE.

It was assumed that small turbulence and nonlinearities at junctions of the capillaries would be negligible. Thus, the resistance R of the FMS (R_{FMS}) was

$$R_{\mathrm{FMS}} = \sum_{l=o}^{s} R_l/N_l \tag{14}$$

Combining eqs 3, 13, and 14 gives

$$R_{\mathrm{FMS}} = \sum_{l=o}^{s} \frac{8\eta L_l}{\pi {r_l}^4 n^l} \tag{15}$$

and yields

$$R_{\mathrm{FMS}} = \frac{(na^4/b)^{s+1} - 1}{(na^4/b) - 1} \frac{R_s}{n^s} \tag{16}$$

where R_s denotes the resistance in level s.

Minimization of the Energy Dissipated in the FMS

The FMS system must assume minimum energy dissipation. As BGE is maintained as it flows through the FMS (eq 12), the corresponding pressure drop was

$$\Delta p = F_{\mathrm{eos},o} R_{\mathrm{FMS}} \tag{17}$$

and the corresponding energy dissipation was

$$W = F_{\mathrm{eos},o}\, \Delta p \tag{18}$$

Combining eqs 17 and 18 gives

$$W = F_{\mathrm{eos},o}^2 R_{\mathrm{FMS}} \tag{19}$$

Equation 19 leads to the conclusion that W energy dissipation

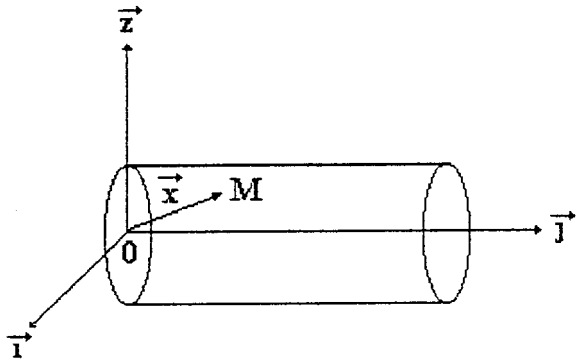

Figure 2. Representation of one capillary. Here, x is the coordinate vector of a point M in the capillary.

depends on the geometrical characteristics r_l, L_l, and n of the FMS: $W(r_l, L_l, n)$.

Following the requirement of the energy minimization principle, this requires the resolution of the following system:

$$\partial W/\partial L_l = \mathrm{O}$$
$$\partial W/\partial r_l = \mathrm{O} \qquad (20)$$
$$\partial W/\partial n = \mathrm{O}$$

Using the standard method of Lagrange multipliers yields the power law

$$a_l = n^{-1/3} \qquad (21)$$

This equation gives the fundamental law for minimizing the energy dissipated in the FMS. The power law $a = n^{-1/3}$, which must be respected, is independent of both the square and circular capillary cross-sections. So far, the electric field strength was assumed to be constant and the voltage across the FMS was not pulsed.

Pulsed Electric Fields

In a Single Capillary. When a pulsed voltage U was applied to the extremities of one capillary, an oscillatory electric field E was created with an angular frequency ω:

$$E = E_\mathrm{o}\, \mathrm{e}^{\mathrm{i}(\omega t - kx)} \qquad (22)$$

where t is time, x is the coordinate vector of a point inside the capillary (Figure 2), and k the wave vector is

$$k = 2\pi/\lambda \qquad (23)$$

Here, λ was the wavelength and E_o the electric field amplitude.

Fused silica has long been the standard material for capillary separations. Recently, several studies have focused on the use of polypropylene,[9−12] polymethacrylate,[13] or fluorinated ethylene-propylene copolymer[15] capillaries as analytical separation tubes for CE.

It is well-known that the mechanical properties of a polymer can be specified by a modulus K which is represented as complex quantities:[25] $K = K' + \mathrm{i}K''$. The real part of K represents the stress component in phase with strain, giving rise to energy storage in the polymer. The imaginary part represents the component of stress which is 90° out of phase with the strain, giving rise to power dissipation in the film. To simplify the problem, the polymeric capillary was considered to be an ideal one, i.e, $K'' = 0$. From eq 22, the oscillatory electric field created a pulsatile electroosmotic flow rate inside the capillary and therefore an oscillatory pressure p:

$$p = p_o\, \mathrm{e}^{\mathrm{i}(\omega t - kx)} \qquad (24)$$

where, p_o is the amplitude average over the radius, $v = \varpi/k$ the wave velocity, and $v_\mathrm{g} = \mathrm{d}\varpi/\mathrm{d}k$ the group velocity. The resistance R in the capillary and v were obtained from well-known Navier Stokes equations.[26] Using the linearized incompressible fluid thin-wall approximation, the term $\xi = (\omega\rho/\eta)^{1/2}r$ (ρ is the density of the BGE) intervenes in the analytical resolution, which gives $R = v_0^2\rho/\pi\, r^2 v$ with $v_0 = (Kh/2\rho r)^{1/2}$ and h the capillary thickness. Two cases can be considered in relation to the r value.

For a Large r Value: Large Capillary. In this case, the parameter ξ is high and the viscosity η of the BGE plays almost no role. Thus, $v = v_0$ and $R = \rho v_0/\pi r^2$ showed that the viscous resistance in the capillary varied with $1/r^2$ and no longer with $1/r^4$ as a nonpulsatile flow.

For a Small r Value: Narrow Capillary. In this case, the role of viscosity η cannot be negligible and $v \rightarrow 0$. The conclusion is that, now, the viscous resistance in the capillary is given by the Poiseuille formula and varies with $1/r^4$ as a nonpulsatile flow.

In the FMS System. The largest tubes were near level 0 ($0 < l < l'$). For these levels, the viscous resistance of a capillary is given as above by $\rho v_0/\pi r_1^2$. Thus, the resistance of the FMS system is given by eq 14, which leads to

$$R_\mathrm{FMS} = \sum_{l=0}^{l'} \frac{\rho v_0}{\pi} \frac{1}{r_1^{\,2}\, n^l} \qquad (25)$$

$$R_\mathrm{FMS} = \frac{(na^2)^{l'+1} - 1}{(na^2) - 1} \frac{R_{l'}}{n^{l'}} \qquad (26)$$

where $R_{l'}$ is the resistance of the level l'. Minimizing the dissipated energy inside the FMS system using the method of Lagrange multipliers, as above, leads to the equation

$$a_{l<l'} = n^{-1/2} \qquad (27)$$

This equation is independent of the capillary cross-section. Equation 27 predicts that the energy-carrying waves are not reflected back up the capillaries at branch points and that the branching is area-preserving. Assuming that the sum of the cross-sectional areas of the daughter branches equal those of the parent (Figure 1) then

$$\lambda\pi r_1^{\,2} = n\lambda\, \pi\, r_{l+1}^2 \qquad (28)$$

yields

$$\frac{r_{l+1}}{r_l} = n^{-1/2} = a_l \qquad (29)$$

As the BGE flows near the smallest tube, the pulsatile flow respects the Poiseuille law (eq 13) and the power law $a_l = n^{-1/3}$ (eq 22) has been restored. These results demonstrate that, for FMS with pulsed flow,

$$l > l'\ a_l = n^{-1/3} \qquad (30)$$

and

$$l < l' \qquad a_l = n^{-1/2} \qquad (31)$$

To minimize the energy dissipated in the FMS, the area must be maintained to respect the largest capillaries. In the other case, the power law $a_l = n^{-1/3}$ must be used. In actual fact, the capillaries used in electrophoresis were usually too small to neglect the viscosity effect (ξ # 0.05) and the Poiseuille law could always be used. Thus, as for a nonpulsatile flow, the power law $a_l = n^{-1/3}$ could be applied to the entire FMS.

In conclusion, the present theoretical study combining energetics with fractal design demonstrates the need to organize the capillaries into a multicapillary electrophoresis system. It was demonstrated that a fractal distribution of the capillaries associated with the power law minimizes the dissipated energy. Practically, the production of energy in CE is the inevitable result of high field strengths. So, effective cooling systems are required to ensure energy removal. The FMS can use high field strengths without too much energy dissipation to perform rapid and efficient separation.

This analysis demonstrates that a pulsatile tension applied to the extremities of an electrophoretic system changed the power law when the cross-section of the capillary was sufficiently large. However, this change cannot be observed because cross-section capillaries are usually too small. To the best of our knowledge, there are no measurements of these effects under the conditions specified here to confirm the predicted trends, but it is anticipated that systematic experimental studies aimed at addressing these issues will appear soon. Our model provides a detailed understanding of the dependence of electroosmotic flow in a pulse hydrodynamic regime; therefore, this model could be a useful starting point for a more refined analysis of multicapillary electrophoresis phenomena.

References and Notes

(1) Slais, K. *J. Chromatogr. A* **1996**, *730*, 247−259.
(2) Cifuentes, A.; Rodriquez, M. A.; Garcia-Montelego, F. J. *J. Chromatogr. A* **1996**, *737*, 243−253.
(3) Cifuentes, A.; Poppe, H. *Electrophoresis* **1995**, *16*, 2051−2059.
(4) Fujimoto, C.; Matsui, H.; Sawada, H.; Jinno, K. *J. Chromatogr. A* **1994**, *680*, 33−42.
(5) Slais, K. J. *Microcolumn Sep.* **1995**, *7*, 127−135.
(6) Burggraf, N.; Manz, A.; Effenhauser, C. S.; Verpoorte, E.; de Rooij, N. F.; Widmer, H. M.; *J. High Resolut. Chromatogr.* **1993**, *16*, 594−596.
(7) Burggraf, N.; Manz, A.; De Rooij, N. F.; Widmer, H. M. *Anal. Methods Instrum.* **1993**, 1, 55−59.
(8) Burggraf, N.; Manz, A.; Verpoorte, E.; Effenhauser, C. S.; Widmer, H. M.; de Rooij, N. F. *Sens. Actuators, B* **1994**, *20*, 103, 110.
(9) Fridstroem, A.; Lundell, N.; Ekstroem, B.; Markides, K. E. *J. Microcolumn Sep.* **1997**, *1*, 9−17.
(10) Ren, X.; Liu, P. Z.; Malik, A.; Lee, M. L. *J. Microcolumn Sep.* **1996**, *8*, 535−540.
(11) Ren, X.; Lin, P. Z.; Lee, M. L.; *J. Microcolumn Sep.* **1996**, *8*, 529−534.
(12) Fridstoem, A.; Markides, K. E.; Lee, M. L. *Chromatographia* **1995**, *41*, 295−300.
(13) Chen, S.; Lee, M. L. *J. Microcolumn. Sep.* **1997**, *9*, 57−62.
(14) Bayer, H.; Engelhardt, H. *J. Microcolumn Sep.* **1996**, *8*, 479−484.
(15) Kaniansky, D.; Zelenska, V.; Baluchova, D. *Electrophoresis* **1996**, *17*, 1890−1897.
(16) Heller, C.; Pakleza, C.; Viovy, J. L. *Electrophoresis* **1995**, *16*, 1423−1428.
(17) Kim, Y.; Morris, M. D. *Anal. Chem.* **1994**, *66*, 3081−3085.
(18) Kim, Y.; Morris, M. D. *Anal. Chem.* **1995**, *67*, 784−786.
(19) Navin, M. J.; Rapp, T. L.; Morris, M. D. *Anal. Chem.* **1994**, *66*, 1179−1182.
(20) Sudor, J.; Novotny, M. *Nucleic Acids Res.* **1995**, *23*, 2538−2543.
(21) Lucas, R. *Kolloid Z.* **1918**, *23*, 15−22.
(22) Washburn, E. W. *Phys. Rev.* **1921**, *17*, 273−283.
(23) Bekely, J.; Neumann A. W.; Chuang, Y. K. *J. Colloid Interface Sci.* **197**1, *35*, 273−278.
(24) Giddings, J. C. *Unified Separation Science*; Wiley: New York, 1991.
(25) Ferry, J. D. *Viscoelastic properties of polymers*, 3rd ed.; Wiley: New York, 1980; Chapter 1.
(26) West, G. B.; Brown, H. J.; Enquist, B. J. *Science* **1997**, *276*, 122−126.